Inorganic Chemistry

Communication

pubs.acs.org/IC

Slow Magnetic Relaxation in a Hydrogen-Bonded 2D Array of Mononuclear Dysprosium(III) Oxamates

Francisco R. Fortea-Pérez,[†] Julia Vallejo,[†] Miguel Julve,*[,†] Francesc Lloret,[†] Giovanni De Munno,[‡] Donatella Armentano,[‡] and Emilio Pardo*[,†]

[†]Departament de Química Inorgànica, Instituto de Ciencia Molecular (ICMOL), Universitat de València, 46980 Paterna, València, Spain

[‡]Dipartimento di Chimica, Università degli Studi della Calabria, CEMIF.CAL, 87030 Cosenza, Italy

Supporting Information

ABSTRACT: The reaction of *N*-(2,6-dimethylphenyl)-oxamic acid with dysprosium(III) ions in a controlled basic media afforded the first example of a mononuclear lanthanide oxamate complex exhibiting a field-induced slow magnetic relaxation behavior typical of single-ion magnets (SIMs). The hydrogen-bond-mediated self-assembly of this new bifunctional dysprosium(III) SIM in the solid state provides a unique example of 2D hydrogen-bonded polymer with a herringbone net topology.

The coordination chemistry of 4f metal ions has experienced a renewed interest because of the relevant role played by lanthanide and actinide complexes in such different fields as catalysis, medical imaging, and materials science.[1] Since the first observation of slow magnetic relaxation effects in double-decker bis(phthalocyaninato)terbium(III) and dysprosium(III) complexes, other examples of mononuclear complexes of lanthanide[2] and transition-metal ions [iron(II) and cobalt(II)][3] have been reported in recent years. Molecules with a single slow-relaxing lanthanide metal center, referred to as lanthanide-based single-ion magnets (Ln SIMs), have been a major scientific target during the past decade because of their potential applications in high-density magnetic memories or quantum computing devices.[1c] That being so, the search for new ligand types that are able to satisfy the coordination (steric and electronic) requirements necessary to get Ln SIMs has currently converted into a hot topic in the field of molecular nanomagnetism. A major goal in this area is the ligand ability to address individual Ln SIMs in crystals and surfaces through weak hydrogen-bonding interactions and/or van der Waals forces.[4]

In our research work concerning the molecular-programmed self-assembly of aromatic polyoxalamide ligands,[5] we prepared the ligand *N*-(2,6-dimethylphenyl)oxamic acid, which can potentially form hydrogen and/or metal−ligand bonds in its different partially or totally deprotonated forms [$H_nL^{(2-n)-}$ with $n = 0-2$; Chart 1a, left] to render the so-called bifunctional metal complexes.[6] As a part of our first exploratory studies on the coordination chemistry of bifunctional lanthanide oxamates, we report herein the synthesis, crystal structure, and magnetic properties of the mononuclear dysprosium(III) complex of formula $Me_4N[Dy^{III}(HL)_4]\cdot 2CH_3CN$ (**1**), where Me_4N^+ is the tetramethylammonium cation (Chart 1, right). Complex **1** exhibits a field-induced slow magnetic relaxation behavior, enlarging thus the scope of Ln SIMs reported in the literature.

Chart 1

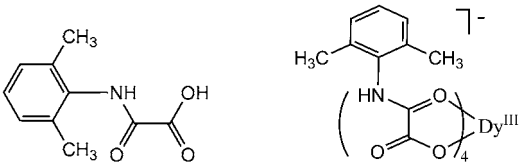

Complex **1** crystallizes in the centrosymmetric space group $P121/n1$ of the monoclinic system. Its structure consists of hydrogen-bonded mononuclear tetrakis(oxamate)dysprosium(III) complex anions with an approximate 2-fold molecular symmetry, $[Dy^{III}(HL)_4]^-$ (Figures 1 and 2), together with tetramethylammonium countercations and acetonitrile molecules of crystallization (Figures S1 and S2, Supporting Information, SI).

The coordination environment of the dysprosium atom in **1** is formed by eight carbonyl oxygen atoms from the carboxamide and carboxylate functions of the four crystallographically independent HL^- ligands in a cis arrangement (Figure 1a). This situation leads to an overall calixarene-type shape for the eight-coordinate anion of **1**, which is reminiscent of that found in the purely organic calixarene analogues, with a mixed outward and inward disposition of the four aromatic substituents [the centroid−centroid distances within the two pairs of directly opposed benzene rings are 5.4 and 11.4 Å] (Figure 1b). The unusual coordination mode for the *O*,*O*′-oxamate chelating ligand can be explained by both the protonated state of the amide nitrogen atom and the preference of rare-earth metal ions for oxygen-donor groups. Analyses of the metal−oxygen bond distances [Dy−O = 2.340(2)−2.407(2) Å] and interbond bite angles [O−Dy−O = 67.36(8)−68.04(7)°] from the chelating oxamate ligands indicate a distorted D_{2d} dodecahedron geometry of the DyO_8 core. In fact, the geometry of the eight-coordinate anion of **1** is characterized by the *quasi*-orthogonal disposition of two almost planar trapezoids defined by two sets of oxygen atoms [O(1)−O(2)−O(10)−O(11)] and [O(4)−O(5)−O(7)−O(8)] (Figure 1c). The values of the dihedral angle (ϕ) between

Received: March 4, 2013
Published: April 18, 2013

   dx.doi.org/10.1021/ic4005517 | *Inorg. Chem.* 2013, 52, 4777−4779

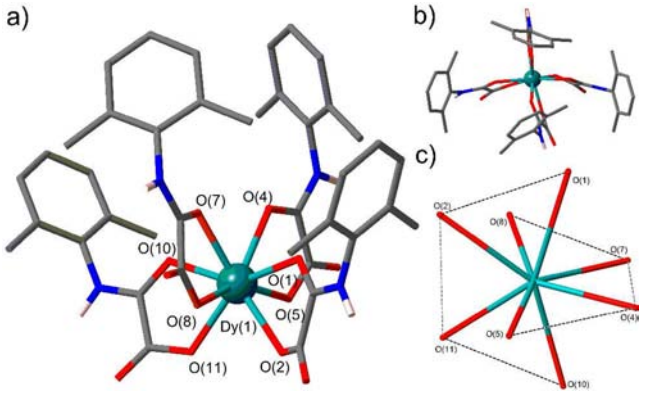

Figure 1. (a and b) Perspective and top projection views, respectively, of the anionic mononuclear dysprosium(III) unit of **1** with the atom-numbering scheme for the metal coordination environment (Dy, green; N, blue; O, red; C, gray; H, pink). Hydrogen atoms from the aromatic substituents are omitted for clarity. (c) View of the metal-coordination polyhedron of **1** showing the two trapezoids from the DyO_8 dodecahedral core. The chelating oxamate ligands are represented by dashed lines.

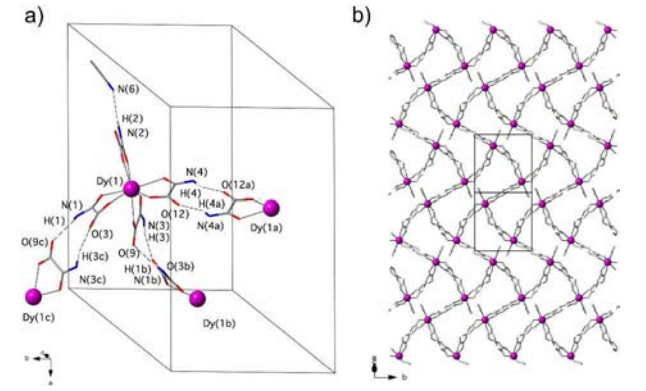

Figure 2. (a) Perspective view of the asymmetric unit of **1** with the atom-numbering scheme [symmetry code: (a) $-x+2, -y, -z+2$; (b) $-x+{}^3/_2, y-{}^1/_2, -z+{}^3/_2$; (c) $-x+{}^3/_2, y+{}^1/_2, -z+{}^3/_2$]. The aromatic substituents are omitted for clarity. Coordination and hydrogen bonds are represented by solid and dashed lines, respectively. (b) Projection view of the hydrogen-bonded layer of mononuclear units of **1** along the [1 0 −1] direction.

the two DyO_2 triangles within each of the two trapezoids are 9.2 and 11.8°, while the value of the twist angle (φ) between the mean planes of the two DyO_4 trapezoids is 87.0°, values which are close to those of an idealized dodecahedron ($\phi = 0°$ and $\varphi = 90°$).[7]

In the crystal lattice of **1**, each mononuclear dysprosium(III) anion, $[Dy^{III}(HL)_4]^-$, is connected to three neighboring ones by double hydrogen bonds between the free amide nitrogen (proton donor) and carbonyl oxygen (proton acceptor) atoms from the carboxamide and carboxylate functions of three chelating oxamate ligands [O···N = 2.801(4)−2.997(3) Å, O···H = 1.91(2)−2.09(2) Å, and O···H−N = 153(4)−164(3)°], while the fourth chelating oxamate ligand establishes a single weak hydrogen bond with one of the crystallization acetonitrile molecules through the free amide nitrogen (proton donor) and nitrile nitrogen (proton acceptor) atoms [N···N = 3.107(4) Å, N···H = 2.25(2) Å, and N···H−N = 155(4)°] (Figure 2a). The hydrogen-bond-mediated self-assembly of these T-shaped supramolecular motifs gives rise to a corrugated "herringbone" rectangular layer of hydrogen-bonded mononuclear dysprosium(III) anions with rather long intermetallic separations [Dy(1)···Dy(1a) = 11.192(1) Å, Dy(1)···Dy(1b) = 10.471(1) Å, and Dy(1)···Dy(1c) = 10.471(1) Å] (Figure 2b). The shortest intermetallic separation [Dy(1)···Dy(1d) = 9.032(1) Å; (d) $2-x, 1-y, 2-z$] within each hydrogen-bonded layer is not related to hydrogen-bonded mononuclear dysprosium(III) anions (Figure S1, SI). The packing of the adjacent layers along the [1 0 −1] direction leads to wide interlayer space, which is occupied by the remaining crystallization acetonitrile molecules and the tetramethylammonium countercations (Figure S2, SI).

The direct-current (dc) magnetic properties of **1** in the form of a $\chi_M T$ versus T plot (χ_M is the dc molar magnetic susceptibility per mononuclear unit) are influenced by the first-order angular momentum and crystal-field effects of the dysprosium(III) ion ($^6H_{15/2}$ term with $S = {}^5/_2$ and $L = 5$; Figure S3, SI). The $\chi_M T$ value of 14.05 $cm^3\ mol^{-1}\ K$ at room temperature is close to that expected for a dysprosium(III) ion [$\chi_M T = (N\beta^2 g^2/3k_B)J(J+1) = 14.15\ cm^3\ mol^{-1}\ K$ with $J = {}^{15}/_2$ and $g = {}^4/_3$]. Upon cooling, $\chi_M T$ first decreases smoothly and then more rapidly below ca. 100 K to reach a value of 11.79 $cm^3\ mol^{-1}\ K$ at 2.0 K. This decrease is due to depopulation of the Stark levels.

The alternating-current (ac) magnetic properties of **1** in the form of χ_M' and χ_M'' versus T plots (χ_M' and χ_M'' are the in-phase and out-of-phase ac molar magnetic susceptibilities per mononuclear unit, respectively) evidence the occurrence of slow magnetic relaxation effects typical of SIMs (Figures 3 and S4−S6, SI). In fact, the absence of a λ peak in the heat capacity measurements of **1** allows us to rule out the occurrence of a 3D long-range magnetic order, thus showing that the mononuclear dysprosium(III) units are magnetically well isolated.

At zero dc magnetic field, both χ_M' and χ_M'' show strong frequency dependence effects below ca. 12 K (Figure S4, SI). However, no maxima of χ_M' and χ_M'' can be observed because of fast quantum-tunneling relaxation, a phenomenon that has already been reported for other SIMs.[2−4] However, when a small dc field such as 250 G is applied, the quantum-tunneling effects are partially suppressed and strong frequency-dependent maxima are observed below ca. 9 K for both χ_M' and χ_M'' (Figure S5, SI). In any case, a divergence in χ_M'' below the blocking temperature still remains, indicating that a quantum-tunneling relaxation mechanism is still operative at 250 G. Additional ac measurements for **1** under higher applied dc fields of 1000 and 2500 G show an almost complete quenching of the fast tunneling relaxation (Figures 3 and S6, SI). Yet, several frequency-dependent satellites besides the main χ_M'' peak can be observed at lower temperatures, suggesting the presence of more than one thermally activated relaxation process when such high dc magnetic fields are applied.

The Cole−Cole plots of **1** at high temperatures under different applied dc fields of 250, 1000, and 2500 G give almost perfect semicircles, which can be fitted by the generalized Debye model (solid lines in the insets of Figures 3b and S5b and S6b, SI).[8a] The small but nonnegligible deviations of the estimated α values (α = 0.12−0.36; Table S2, SI) with respect to that expected for a Debye model ($\alpha = 0$) agree with the occurrence of more than one relaxation process.[8b] Moreover, the values of the relaxation time of **1**, which are calculated from the maximum of χ_M'' at a given frequency ($\tau = 1/2\pi\nu$), follow the Arrhenius law characteristic of a thermally activated mechanism [$\tau = \tau_0 \exp(E_a/k_B T)$] (solid lines in the insets of Figures 3a and S5a and S6a, SI). The calculated values of the preexponential factor [$\tau_0 = (2.06-4.35) \times 10^{-10}$ s] and the activation energy ($E_a = 49.8-65.1\ cm^{-1}$; Table

dx.doi.org/10.1021/ic4005517 | Inorg. Chem. 2013, 52, 4777−4779

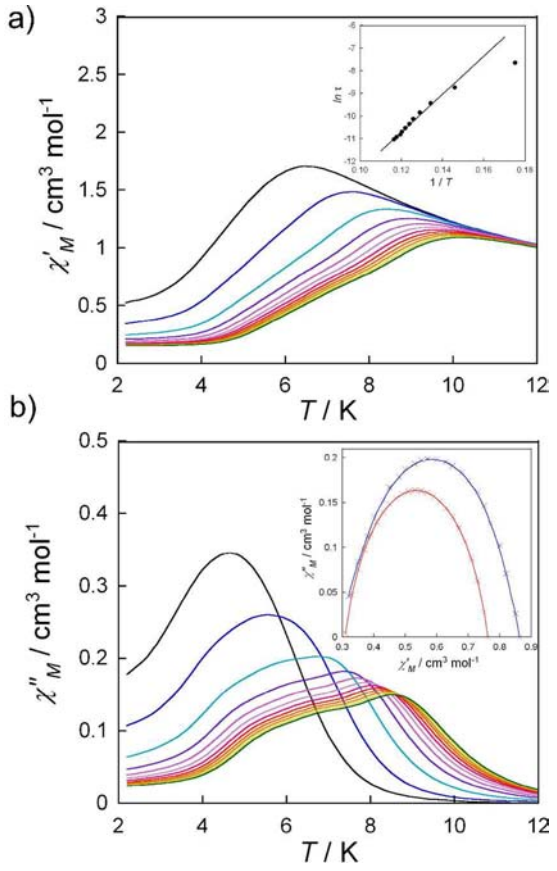

Figure 3. Temperature dependence of χ_M' (a) and χ_M'' (b) of **1** under an applied dc field of 1000 G in the frequency range of 300 (green)−10000 (black) Hz. The solid lines are only eye-guides. The insets show the (a) Arrhenius and (b) Cole−Cole plots at 8 (blue) and 9 (red) K. The solid lines are the best-fit curves (see the text).

S3, SI) are consistent with those previously reported for other Ln SIMs with multiple relaxation processes.[2h,i] The occurrence of quantum-tunneling relaxation effects is most likely responsible for deviations from linearity of the Arrhenius plots in the low-temperature region.

In conclusion, a mononuclear dysprosium(III) complex exhibiting a unique hydrogen-bond-directed self-assembly process in the solid state has been synthesized from a suitable aromatic-substituted oxamate ligand that can simultaneously form metal−ligand and hydrogen bonds. This novel mononuclear dysprosium(III) complex is the first example of an oxamato-based Ln SIM, enlarging thus the scope of slow-relaxing molecular magnetic materials of the well-known oxamato family.[5] Current efforts are devoted to investigating the possible influence of the intermolecular hydrogen-bonding interactions on the observed multiple slow magnetic relaxation behavior of this unique bifunctional Ln SIM.

■ ASSOCIATED CONTENT

Ⓢ Supporting Information

Preparation and physical characterization data and crystallographic refinement details of **1**, Tables S1−S3, Figures S1−S6, and a CIF file for **1** (CCDC 921556). This material is available free of charge via the Internet at http://pubs.acs.org.

■ AUTHOR INFORMATION

Corresponding Author

*E-mail: Emilio.Pardo@uv.es (E.P.), Miguel.Julve@uv.es (M.J.).

Notes

The authors declare no competing financial interest.

■ ACKNOWLEDGMENTS

This work was supported by the MICINN (Spain; Project CTQ2010-15364), the University of Valencia (Project UV-INV-AE11-38904), and the Generalitat Valenciana (Spain; Projects PROMETEO/2009/108, GV/2012/051, and ISIC/2012/002). F.R.F.-P., J.V., and E.P. thank the MICINN for contracts.

■ REFERENCES

(1) (a) Edelman, F. T. *Chem. Soc. Rev.* **2012**, *41*, 7567. (b) Werner, E. J.; Datta, A.; Jocher, C. J.; Raymond, K. N. *Angew. Chem.* **2008**, *47*, 8568. (c) Sessoli, R.; Powell, A. K. *Coord. Chem. Rev.* **2009**, *253*, 2328.

(2) (a) Ishikawa, N.; Sugita, M.; Ishikawa, T.; Koshihara, S.-Y.; Kaizu, S. *J. Am. Chem. Soc.* **2003**, *125*, 8694. (b) Ishikawa, N.; Sugita, M.; Ishikawa, T.; Koshihara, S.; Kaizu, S. *J. Phys. Chem. B* **2004**, *108*, 11265. (c) Rinehart, J. D.; Long, J. R. *J. Am. Chem. Soc.* **2009**, *131*, 12558. (d) Chilton, N. F.; Langley, S. K.; Moubaraki, B.; Soncini, A.; Batten, S. R.; Murray, K. S. *Chem. Sci.* **2013**, *4*, 1719. (e) Layfield, R. A.; McDouall, J. J. W.; Sulway, S. A.; Tuna, F.; Collison, D.; Winpenny, R. E. P. *Chem.—Eur. J.* **2010**, *16*, 4442. (f) Cucinotta, G.; Perfetti, M.; Luzon, J.; Etienne, M.; Car, P.-E.; Caneschi, A.; Calvez, G.; Bernot, K.; Sessoli, R. *Angew. Chem.* **2012**, *124*, 1638. (g) Jeletic, M.; Lin, P.-H.; Le Roy, J. J.; Korobkov, I.; Goelsky, S. I.; Murugesu, M. *J. Am. Chem. Soc.* **2011**, *133*, 19286. (h) Car, P.-E.; Perfetti, M.; Mannini, M.; Favre, A.; Caneschi, A.; Sessoli, R. *Chem. Commun.* **2011**, *47*, 3751. (i) Ruiz, J.; Mota, A. J.; Rodríguez-Diéguez, A.; Titos, S.; Herrera, J. M.; Ruiz, E.; Cremades, E.; Costes, J. P.; Colacio, E. *Chem. Commun.* **2012**, *48*, 7916.

(3) (a) Freedman, D. E.; Harman, W. H.; Harris, T. D.; Long, G. J.; Chang, C. J.; Long, J. R. *J. Am. Chem. Soc.* **2010**, *132*, 1224. (b) Lin, P.-H.; Smythe, N. C.; Gorelsky, S. I.; Maguire, S.; Henson, N. J.; Korobkov, I.; Scott, B. L.; Gordon, J. C.; Baker, R. T.; Murugesu, M. *J. Am. Chem. Soc.* **2011**, *133*, 15806. (c) Zadrozny, J. M.; Long, J. R. *J. Am. Chem. Soc.* **2011**, *133*, 20732. (d) Jurca, T.; Farghal, A.; Lin, P.-H.; Korobkov, I.; Murugesu, M.; Richardson, D. S. *J. Am. Chem. Soc.* **2011**, *133*, 15814. (e) Vallejo, J.; Castro, I.; Ruiz-García, R.; Cano, J.; Julve, M.; Lloret, F.; De Munno, G.; Wernsdorfer, W.; Pardo, E. *J. Am. Chem. Soc.* **2012**, *134*, 15704.

(4) Jeon, I.-R.; Clérac, R. *Dalton Trans.* **2012**, *41*, 9569.

(5) Dul, M. C.; Pardo, E.; Lezcouëzec, R.; Journaux, Y.; Ferrando-Soria, J.; Ruiz-García, R.; Cano, J.; Julve, M.; Lloret, F.; Cangussu, D.; Pereira, C. L. M.; Stumpf, H. O.; Pasán, J.; Ruiz-Pérez, C. *Coord. Chem. Rev.* **2010**, *254*, 2281.

(6) (a) Burrows, A. D.; Chan, C. M.; Chowdhry, M. M.; McGrady, J. E.; Mingos, D. M. P. *Chem. Soc. Rev.* **1995**, *24*, 329. (b) Tadokoro, M.; Nakasuji, K. *Coord. Chem. Rev.* **2000**, *198*, 205.

(7) Cotton, F. A.; Murillo, C. A.; Wang, X. *Inorg. Chim. Acta* **2000**, *300−302*, 1.

(8) (a) Cole, K. S.; Cole, R. H. *J. Chem. Soc.* **1941**, *9*, 341. (b) Mydosh, J. A. *Spin Glasses: An Experimental Introduction*; Taylor & Francis: London, 1993.

dx.doi.org/10.1021/ic4005517 | *Inorg. Chem.* 2013, 52, 4777−4779